A New Approach for the Estimation of Longitudinal Damping Derivatives: CFD Validation on NACA 0012

PIERO GILI
Polytechnic of Turin
DIMEAS
C.so Duca degli Abruzzi 24
ITALY
piero.gili@polito.it

MICHELE VISONE
Blue Engineering
AeroThermal CFD Manager
Via Albenga 98
ITALY
m.visone@blue-group.it

ANGELO LERRO
Italsystem srl
Research Manager
Via Aldo Pini
ITALY
a.lerro@italsystemsrl.it

FRANCESCO DE VIVO
Univ. of Naples Federico II
Master's Degree
ITALY
devivo.francesco@virgilio.it

GIANLUCA SCOGNAMIGLIO
CNH Industrial
Design Project Engineer
ITALY
gianluca.scognamiglio@cnhind.com

Abstract: Aerodynamic longitudinal damping derivatives are of great importance for aircraft stability and control and for aircraft aeroelasticity problems. The classical methods adopted to calculate damping derivatives, using USAF Datcom or wind tunnel tests, are not accurate enough for unconventional shaped aircrafts in particular. Moreover, experimental methods refer to body pitch and plunge motion: it follows that the derivatives are affected to a great extent by the frequency. Some authors have proposed quasi-steady methods, which fail at the transonic regime. To overcome all of these shortcomings, a new approach, based on looping and heaving motion, is presented. The results of the proposed methods are validated, using CFD simulation with the NACA 0012 airfoil, against the exact Theodorsen theory, indicial functions and numerical results from other authors.

Key–Words: Damping derivatives, CFD, Flight mechanics, Moving boundary.

Nomenclature

Re	Reinold Number
M	Mach Number
V_∞	freestream velocity, [m/s]
c	airfoil chord, [m]
t	time, [s]
T	time period, [s]
ω	frequency, [rad/s]
K	reduced frequency, $\omega c/2V_\infty$
α	angle of attack
β	sideslip angle
h	translational vertical velocity, [m/s]
p, q, r	angular rate components, [rad/s]
C_d	drag cefficient
C_l	lift cefficient
C_m	pitching moment coefficient
C_n	normal force cefficient
$C_{m_{ac}}$	pitching moment coefficient w.r.t. the ac
$C_{l,\dot\alpha}$	coefficient derivative $\partial C_l/\partial(c\dot\alpha/2V_\infty)$
$C_{d,\dot\alpha}$	coefficient derivative $\partial C_d/\partial(c\dot\alpha/2V_\infty)$
$C_{m_{ac},\dot\alpha}$	coefficient derivative $\partial C_{m_{ac}}/\partial(c\dot\alpha/2V_\infty)$
$C_{n,\dot\alpha}$	coefficient derivative $\partial C_n/\partial(c\dot\alpha/2V_\infty)$
$C_{l,q}$	coefficient derivative $\partial C_l/\partial(cq/2V_\infty)$
$C_{d,q}$	coefficient derivative $\partial C_d/\partial(cq/2V_\infty)$
$C_{m_{ac},q}$	coefficient derivative $\partial C_{m_{ac}}/\partial(cq/2V_\infty)$

1 Introduction

The present work arose from the need to evaluate the dynamics and new autopilot performances of unconventional-shaped aircraft, such as modern UAVs, during the design stage. The need to have suitable commands, reliable flight controls and flight simulators for pilot training before the first flights is one of the most important keys to success when designing an unmanned aircraft. For this purpose, predicting flight dynamics, or in other words, calculating the classical and the dynamic derivatives with a good precision, is of fundamental importance. The present work has only been focused on longitudinal dynamics for two reasons: first, longitudinal and lateral direc-

tional dynamics can be considered uncoupled, within certain limits [4]. Second, because the contents of this article are not limited to longitudinal dynamics and can easily be extended to lateral directional dynamics, even in the case of cross-coupling of the dynamics. Therefore the first aim of this work was to propose a general validity methodology, with no regime limitations, that can also be used during the design stage, if coupled to a numerical code. The approach is based on steady state maneuvers for the looping derivative and on time consistent motion for the pitch-damping derivatives, but with no frequency effects. The second aim of this work was to validate the approach using a commercial CFD code and the NACA0012 airfoil because of the large amount of literature that is available about it. After introducing the state of the art on dynamic derivative calculation, the approach will be presented and analytically demonstrated under the hypothesis of the superposition principle and, after a brief description of the numerical simulations, the validation of the methodology will be presented.

2 Description of the method

Damping derivatives govern longitudinal aircraft dynamics [12]. In the case of uncoupled dynamics and small disturbance hypothesis, the perturbed longitudinal equation may be expressed as

$$\begin{Bmatrix} C_d \\ C_l \\ C_m \end{Bmatrix} = \begin{bmatrix} C_{d,\alpha} & C_{d,\dot{\alpha}} & C_{d,q} \\ C_{l,\alpha} & C_{l,\dot{\alpha}} & C_{l,q} \\ C_{m,\alpha} & C_{m,\dot{\alpha}} & C_{m,q} \end{bmatrix} \begin{Bmatrix} \alpha \\ \dot{\alpha} \\ q \end{Bmatrix}. \quad (1)$$

Two different kinds of motion have been considered to evaluate all the damping longitudinal derivatives $C_{l,\dot{\alpha}}$, $C_{d,\dot{\alpha}}$, $C_{m,\dot{\alpha}}$, $C_{l,q}$, $C_{d,q}$, $C_{m,q}$ and for several attitudes: the heaving and the looping motion performed varying the angle of attack. For the heaving motion shown in Figure 1, the airfoil, or more in general, the body, is animated by a vertical descent motion with constant acceleration, $\ddot{h}$, or, in other words, with a constant pitching velocity, (see Eq. 2), so that the flow field is characterized by null q and variable $\dot{\alpha}$ as a result of the composition of the asymptotic flow velocity and vertical body velocity, according to Eq. 2.

$$\alpha(t) = \arctan\left(\frac{\dot{h}_{fluid}}{V_x}\right). \quad (2)$$

Usually, the aerodynamic coefficients can be expressed as a linear combination of several contributions, for example, the lift coefficient can be expressed

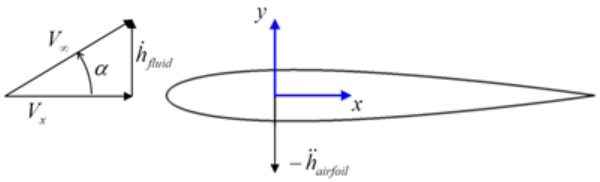

Figure 1: Heaving motion for the CFD model obtained through superimposition of the asymptotic velocity and constant vertical acceleration.

as

$$C_l(t) = C_{l,\alpha}\alpha(t) + C_{l,\dot{\alpha}}[\alpha(t), \dot{\alpha}]\dot{\alpha} \quad (3)$$

where the pitch damping coefficient, $C_{l,\dot{\alpha}}$, has been expressed in its most general non-linear form. Moment and drag coefficients have the same structure.

Therefore, in order to obtain a maneuver with a constant pitch velocity, $\dot{\alpha} \approx \ddot{h}/V_\infty$, and null angular velocity, $q = 0$, it is necessary to move the airfoil in the vertical direction with a constant acceleration, which is equivalent to superimposing a linear time-increasing vertical velocity, $\dot{h}$. This motion, as previously mentioned, produces a time varying α, but the convenience of this motion is that all the higher order contributions of the angle of attack are null, $d^n\alpha/dt^n = 0\,\forall n \geq 2$. Therefore, the only two contributions to aerodynamics are α and $\dot{\alpha}$. Obviously, the heaving maneuver requires relative motion between the airfoil motion and the base flow.

As will be shown, if the heaving maneuver is repeated at different values of $\dot{\alpha}$, the $\dot{\alpha}$ contribution can easily be calculated by subtracting the steady state contribution, $C_{l,\alpha}(t)$, from the resulting coefficient, $C_l(t)$. The derivative is then obtained by dividing the contribution by the constant pitching velocity, $\dot{\alpha}$.

The looping maneuver can be used to isolate the effect of looping velocity, q, since the angle of attack, α, is fixed and calculated at the quarter chord, as shown in Figure 2. Moreover, there is no contribution of $\dot{q}$ or higher order terms, therefore this maneuver can be performed by simply giving curvature to the flow field. This time, the aerodynamic coefficients are expressed in terms of the looping derivatives, as follows

$$C_l(t) = C_{l,\alpha}\alpha(t) + C_{l,q}[\alpha(t)]q \quad (4)$$

where the looping damping coefficient, $C_{l,q}$, has been expressed in its most general form. If the heaving maneuver is repeated at different values of q, the contribution can easily be calculated by subtracting the steady state contribution, $C_{l,\alpha}(t)$, from the resulting coefficient, $C_l(t)$. The derivative is then obtained by

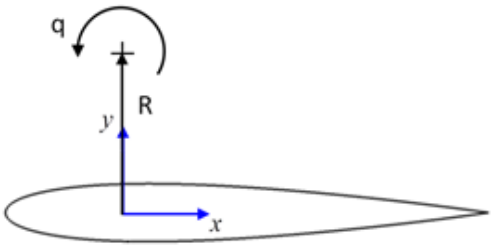

Figure 2: Looping motion for the CFD model obtained with a constant rate velocity.

dividing the aerodynamic coefficient contribution by the constant looping velocity, q.

2.1 Mathematical model

CFD simulations have been carried out using the commercial CFD code, STAR-CCM+, which solves the complete set of Navier-Stokes equations with the finite volume method under the hypothesis of a non inertial reference frame. All the simulations were computed for the NACA 0012 airfoil at $Re = 2.5-3\times10^6$ and with a null Mach number. Moreover, two turbulence models were considered. The fully turbulent simulations were performed using the $k-\omega$ without the transition model, the same $k-\omega$ two-equation model was also used with the $\gamma - Re_\Theta$ transition model, which was necessary to evaluate the influence of the transition and laminar separation, which also occurs for static analysis for $\alpha > 5.5°$ [5], on dynamic simulations. The simulation settings were settled as suggested by Malan et al [10]. The Unsteady RANS equations were solved using a sequential algorithm based on the SIMPLE method with a second order discretization model. The time step was chosen, in the time implicit algorithm, in order to obtain a convective Courant number no greater than 10. The computational domain dimensions and the boundary conditions are reported in Figure 3. The velocity inlet condition was imposed on all boundaries to overcome some issues related to the combination of pressure and the moving reference.

Three C-type structured grids have been generated in order to perform a sensitivity analysis in the presence of moving boundaries and a transition model. The mesh details are reported in Table 1.

Mesh	Points on the airfoil	Grid points
coarse	150	275×90
medium	200	400×110
fine	300	550×130

Table 1: Mesh adopted to perform the sensitivity analysis.

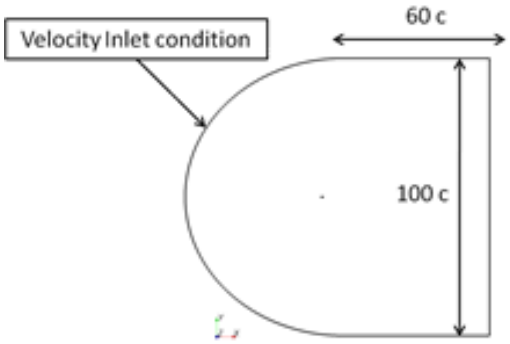

Figure 3: Computational domain dimensions and boundary conditions.

The details of the airfoil mesh are shown in Figure 4.

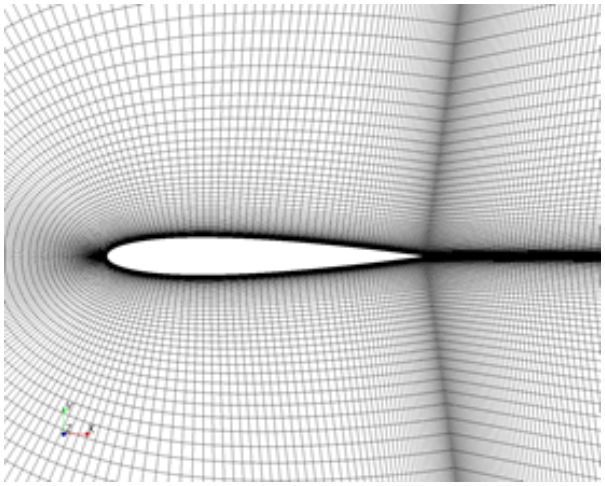

Figure 4: Medium (400×170) near view.

The relative motion between the flow field and the airfoil has been simulated considering a moving (or non-inertial) reference frame. Star-CCM+ offers the possibility of physically moving grid points during transient analysis. With a moving reference frame activated, the equations of motion are modified to incorporate the additional acceleration terms that occur due to the transformation from the stationary to the moving reference frame [2]. The unsteady heaving motion has been obtained using the unsteady moving boundary technique, RBM (Rigid Body Motion) that is available in Star-CCM+. The looping motion, which does not require relative motion between the flow field and the body, but only a constant curvature of the base flow, has instead been simulated using the stationary moving reference frame technique, MRF (moving reference frame) that is available in Star-CCM+.

3 Validation

The method here presented claims to calculate all the longitudinal derivatives using looping and heaving maneuvers, and it was decided to use CFD to validate the method. It was therefore necessary to validate the CFD model with both steady and unsteady well documented test cases. Three different grid meshes (coarse, medium and fine) were generated and compared with the selected references. Figure 5 and 7 show that the medium grid mesh is the best compromise between static solution accuracy and computational weight, on the basis of a comparison with experimental [1, 7].

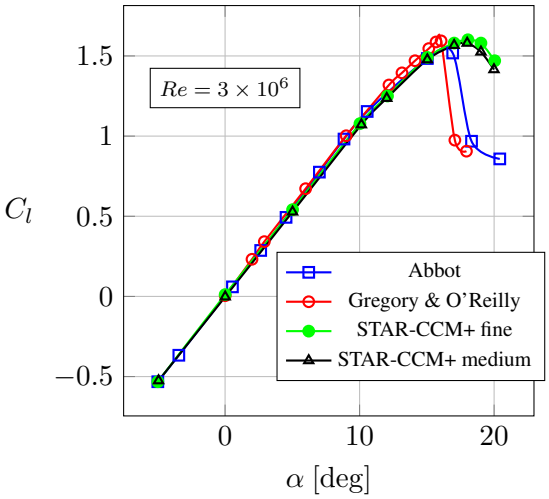

Figure 5: Static lift coefficient

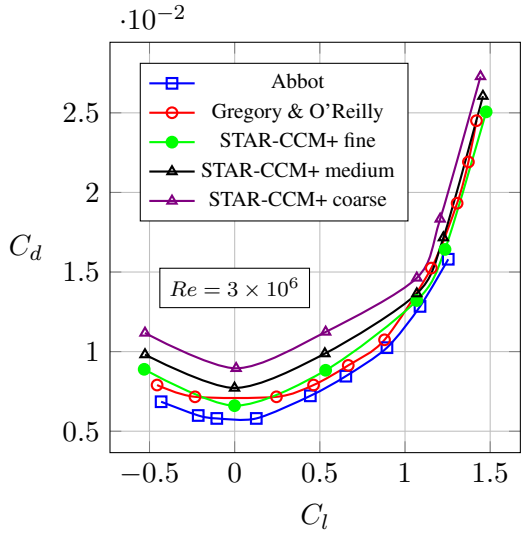

Figure 6: Static drag coefficient

The unsteady validation was first performed to establish whether the medium mesh grid had the same accuracy with an unsteady validation and then to evaluate the difference in aerodynamic forces with and without the transition model. This issue has been evaluated because, the authors are not looking for the exact aerodynamic forces on oscillating airfoils in this work, but, as previously mentioned, just want to set up a CFD model that is able to give suitable results in order to validate the here presented methodology. Moreover, since the here presented method is of general validity and is not related to CFD, it can be exploited in any feasible way. Pitching motion [11], with $\alpha(t) = 11 + 6\sin(\omega t)$, $Re = 2.5 \times 10^6$, $M = 0.09$ and $K = 0.24$, has been considered in order to evaluate the performance and suitability of the CFD model when the airfoil is simulated outside the linear range of the lift curve. The purpose of this comparison is firstly to validate the CFD model for the NACA 0012 airfoil and then to evaluate the importance of the transition model for this kind of simulation.

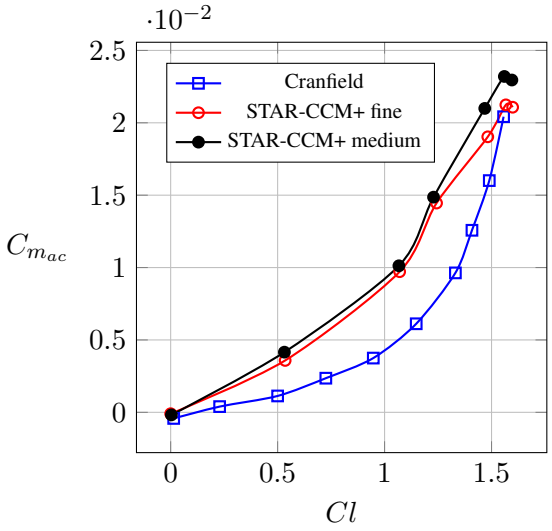

Figure 7: Static pitching moment coefficient

From Figure 8 and 9 it emerges that the medium grid mesh is both accurate in predicting unsteady aerodynamic forces and that there are no important differences when using or not the transition model. This is due to the fact that the laminar separation on the leading edge of the NACA 0012 airfoil [5, 7] is quite stable and does not cause stall because of laminar separation, as was also observed by Ashraf et al [3]. Therefore, the use of the medium mesh grid and a fully turbulent flow is the best and lightest approach to validate the here presented methodology.

4 Results

The results of the non-linear heaving and looping motion will be shown in this section. The longitudinal damping derivative has been calculated starting from

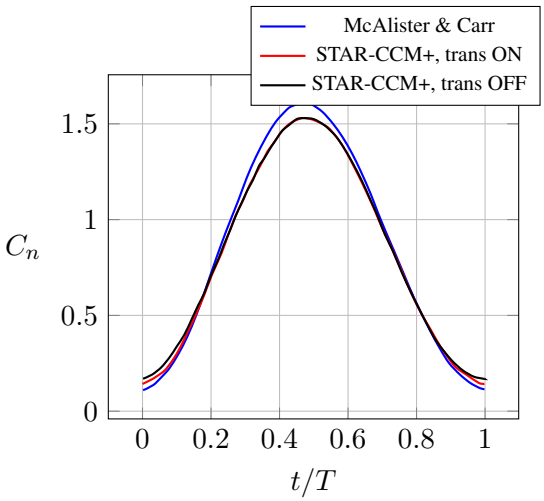

Figure 8: Normal force coefficient comparison between experimental results [11] and numerical simulation with and without transition.

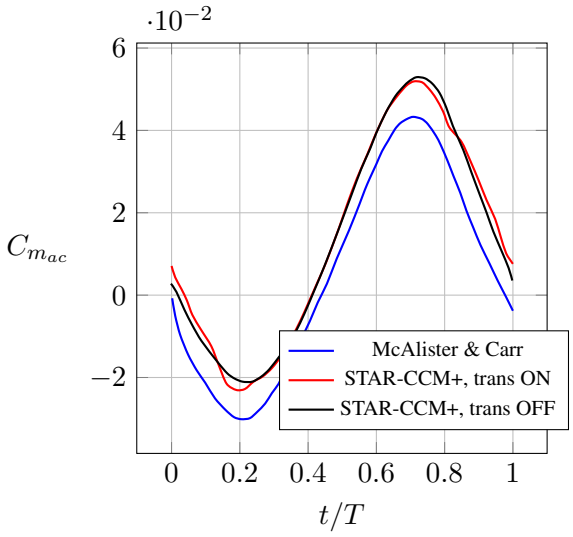

Figure 9: Moment coefficient comparison between experimental results [11] and numerical simulation with and without transition.

Eqs. 3 and 4, subtracting the steady state value of the corresponding aerodynamic quantities, obtained with static simulations, to obtain the aerodynamic coefficient dynamic contributions, and then dividing these dynamic contributions by the value of the animating variable that was considered, q or $\dot{\alpha}$.

4.1 Heaving

The novelty of this paper is that the angle of attack prime derivative calculation, a direct calculation, without any influence of other variables, is feasible as will be shown in this section. The results of the heaving motion presented in a previous section, with constant vertical acceleration, $\ddot{h}$, or equivalently the angular rate, $\dot{\alpha}$, are plotted and compared with the analytical value of the indicial function [14] for the lift force shown in Figure 10 and 11. As far as the indicial function is concerned, it is necessary to point out that the value considered here has been approximated to the function [4] in Eq. 5

$$\phi(t) = 1 - 0.165e^{-0.0455\tau} - 0.335e^{-0.3\tau} \qquad (5)$$

As is well known, the indicial functions for an airfoil are derived by approximating the Wagner function [15], which is the basis of the Theodorsen theory [13] that is not approximated. Therefore, the indicial functions approximate the Theodorsen theory, but also offer the great advantage of being very easy to implement and develop for any aerodynamic body if compared to the Theodorsen formulation. Here, the indicial function is compared with the time evolution of the aerodynamic coefficients, while the Theodorsen results are presented in terms of the derivatives, since it is rather easy to derive analytical derivative expressions, bearing in mind that they are two sides of the same coin, that is, the Wagner formulation.

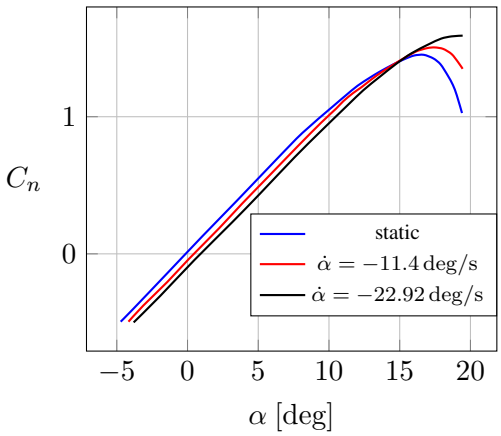

Figure 10: Static C_n and heaving C_n

Figure 10 shows the difference between the steady state lift profile and time consistent heaving motion. The presence of heaving motion lowers the zero lift axis and delays the stall to higher angles of attack, in agreement with what has been observed by other authors [8]; the higher the heaving velocity, the higher the stall angles. Figure 11 shows a comparison between the analytical value derived from Theodorsen's exact theory, and the results of the indicial function and numerical simulation. It can be noticed that the derivative is quite constant within the linear lift range, and in good agreement with the Theodorsen analytical value, and that the derivative

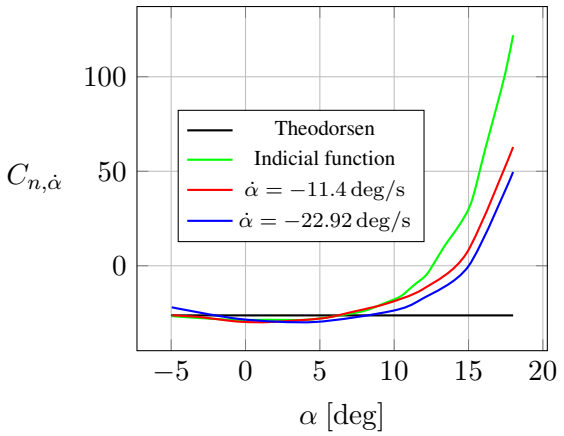

Figure 11: Normal force derivative due to $\dot{\alpha}$

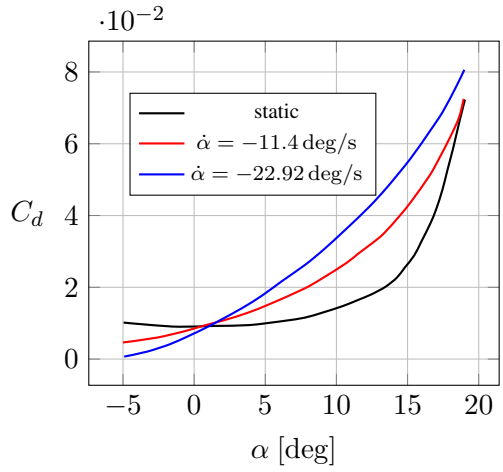

Figure 12: Static C_d and heaving C_d

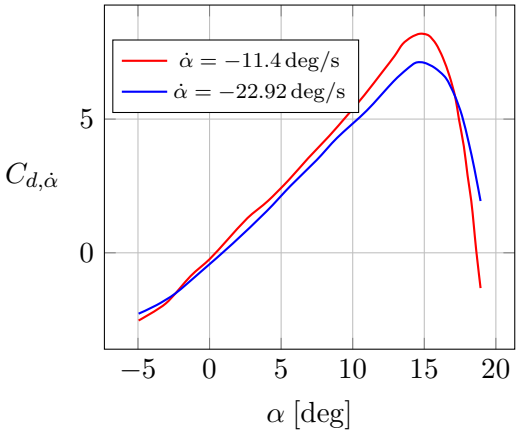

Figure 13: Drag force derivative due to $\dot{\alpha}$

and sign change to a great extent outside the linear range. The numerical simulation is a little more accurate than the indicial prediction for high lift because only a linear indicial function (see Eq. 5) has been considered. Non linear indicial functions should be used to improve the accuracy of the indicial formulation, but the drawback, the necessity of calculating these functions in the high lift region, would be reintroduced. The heaving maneuver, here presented and reproduced exploiting numerical simulations, is able to predict the value of both small and high angles of attack, and offers the opportunity of parameterizing the derivatives while varying the angle of attack, α, and the pitching velocity, $\dot{\alpha}$. The drag force results are shown in Figure 12 and 13 and the moment evaluated at a quarter chord are given in Figure 14 and 15. The moment pitching derivative, $C_{m_{ac},\dot{\alpha}}$, is constant for $\alpha < 5°$ and then changes considerably. The minor differences between the theoretical and numerical values are due to the turbulent drag force which, obviously, is not taken into account in the Theodorsen theory or in the present linear indicial function. The good comparison between the numerical and theoretical data validates this methodology, which exploits the heaving maneuver, to calculate the pitch damping derivative when only the pitching velocity, $\dot{\alpha}$, is excited.

4.2 Looping

In order to complete the longitudinal damping derivative set ($\dot{\alpha}$ and q derivatives), the looping motion has been performed to calculate the looping velocity, q, contribution. The maneuvers have been repeated for several angles of attack and extended to stall; the results are plotted in Figure 16, 18 and 19.

It can be observed that the lift coefficient slope is quite constant while the stall is promoted by the looping velocity. The lift and moment coefficients are influenced to great extent by the pitch rate, and it can be noticed that the higher the pitch rate, the sooner stall occurs. It can be noticed from Figure 17 that the lift looping derivative, $C_{l,q}$, is quite constant for very small angles of attack ($\alpha < 10°$), but if the angle of attack,α, is increased the derivative decreases significantly and it also changes sign. The drag coefficient is not influenced to any extent by the looping velocity, as is well known [6, 12], and it is plotted in Figure 18

Figure 20 shows that the moment coefficient looping derivative, $C_{m,q}$, is almost constant for small angles of attack ($\alpha < 10°$), while it increases significnatly for higher angles of attack. The minor differences between theoretical and numerical values are due to the effect of turbulent drag force. A comparison between the results of the present work, considering angles of attack from 0 to 15°, the Theodorsen theory and Limache and Cliff simulations [9], which are computed at a zero angle of attack, is shown in Figure 17 and 20. It can be seen that there is very good agreement

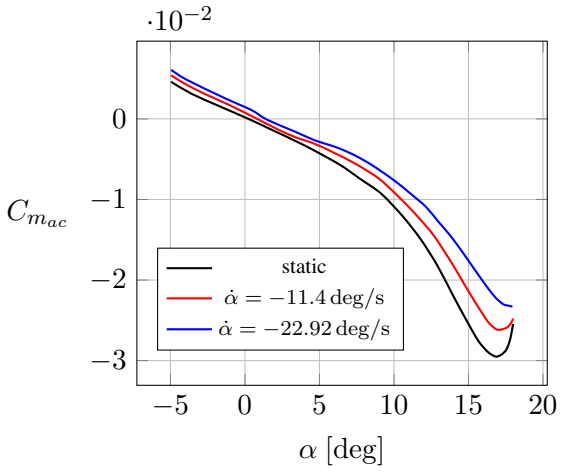

Figure 14: Static $C_{m_{ac}}$ and heaving $C_{m_{ac}}$

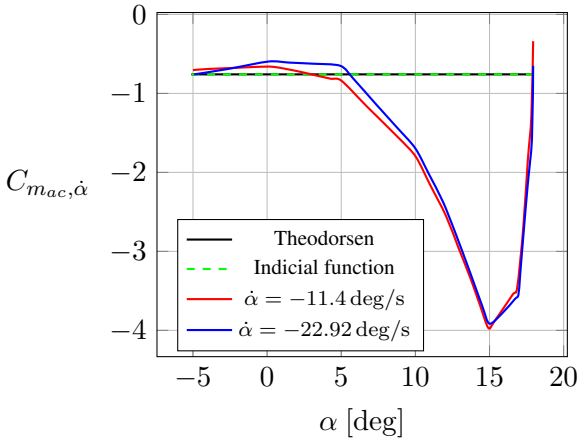

Figure 15: Moment derivative due to $\dot{\alpha}$

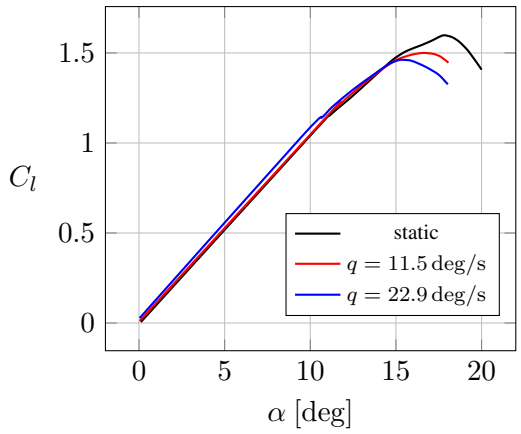

Figure 16: Lift force coefficient due to q

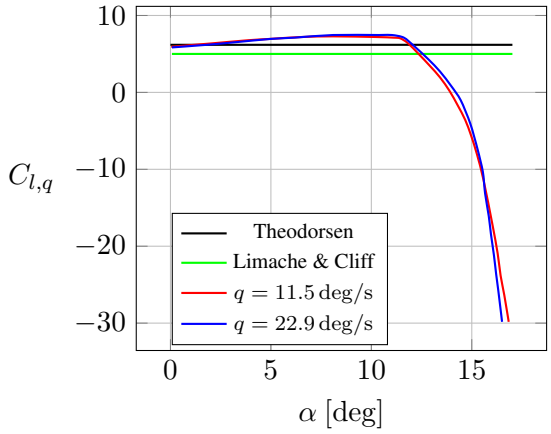

Figure 17: Lift coefficient derivative with respect to q

between the Theodorsen linear theory and CFD simulations for angles of attack of less than $10°$. If the looping velocity and angle of attack are increased, a considerable variation of the lopping derivatives can be observed, which cannot be neglected.

5 Conclusion

In this work, a brief introduction has been given on the state of the art of the calculation of damping derivatives, and the advantages and drawbacks of the different methodologies have been pointed out. The aerodynamic response of the NACA 0012 airfoil has been investigated for heaving and looping maneuvers, respectively, and for unsteady and steady numerical simulations, using the commercial CFD Star-CCM+ code, with the aim of evaluating the longitudinal damping derivatives. The here proposed methodology has been described and then analytically demonstrated under the hypothesis of the superposition principle. The looping and heaving maneuvers used for the longitudinal damping derivative calculation and the way of calculating these derivatives have also been described. The results have been reported, and they show very good agreement with the analytical values of the indicial function, with the Theodorsen theory and with other CFD methods used for looping simulations. Therefore, the results show that the here presented method is useful when a complete set of longitudinal damping derivatives is needed, and it is able to give information at any attitude, according to the limits of the instruments (CFD, experimental end so forth) used to simulate the maneuvers. The here presented methodology shows a general validity and is not linked to CFD, but it can be exploited by any other technique. The proposed technique, if used with CFD codes, is rather cheap because it does not need any remeshing or deforming mesh, but exploits meshes already set up for conventional aerodynamic analysis. Moreover, although the pitching derivatives need time consistent simulations, the looping derivatives can be calculated through a simple steady state analysis, as

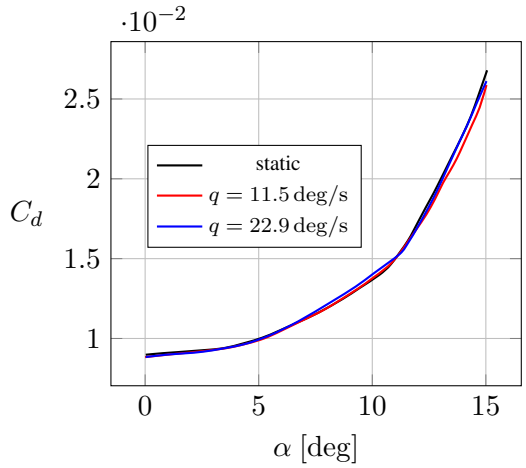

Figure 18: Static C_d and looping C_d

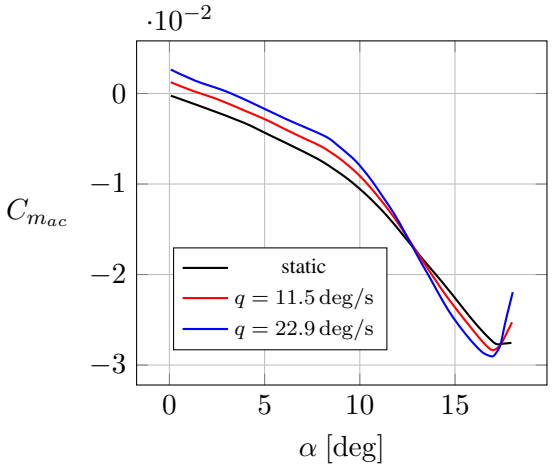

Figure 19: Static C_m and heaving C_m

shown for the looping maneuver. In short, the methodology here presented can easily be extended to lateral directional dynamics, which will be the subject of future work.

References:

[1] I.H. Abbott and A.E. Von Doenhoff. *Theory of Wing Sections: Including a Summary of Airfoil Data*. Dover Publications, 1959.

[2] CD-ADAPCO. *STAR-CCM+, User Guide*. 5.02. STAR. 2009.

[3] M. A. Ashraf, J.C.S. Lai, and M.F. Platzer. "Aerodynamic Analysis of Flapping-Wing Propellers For HALE Aircraft". In: *47th AIAA Aerospace Sciences Meeting* (2009).

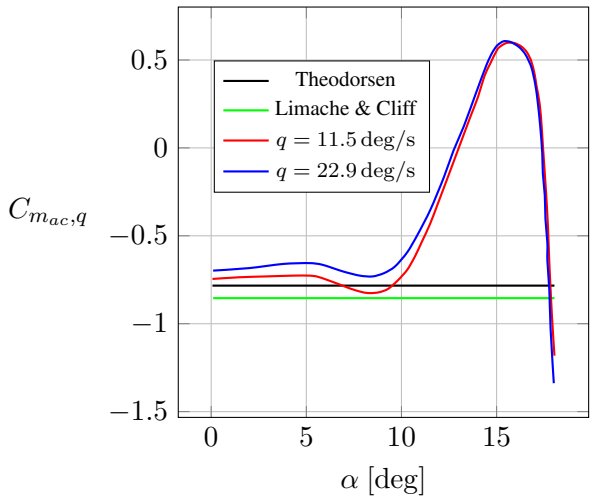

Figure 20: Moment derivative due to q

[4] R.L. Bisplinghoff, H. Ashley, and R.L. Halfman. "Aeroelasticity". In: *Dover Publications* (1996).

[5] H.A. Dwyer and W.J. Aiccroskey. "Crossflow and Unsteady Boundary-Layer Effects on Rotating Blades". In: *AIAA Journal* 9.8 (1971), pp. 1498–1505.

[6] B. Etkin and L.D. Reid. *Dynamics of Flight: Stability and Control*. Wiley, 1996.

[7] N. Gregory and C.L. O'Reilly. *Low-speed Aerodynamic Characteristics of NACA 0012 Aerofoil Section, Including the Effects of Upper-surface Roughness Simulating Hoar Frost*. Tech. rep. National Physical Laboratory, 1970.

[8] N.D. Ham. "Aerodynamic Loading on a Two-Dimensional Airfoil during Dynamic Stall". In: *AIAA Journal* 6.10 (1968), pp. 1927–1934.

[9] A.C. Limache and E.M. Cliff. "Aerodynamic Sensitivity Theory for Rotary Stability Derivatives". In: *AIAA Paper* 98.4313 ().

[10] P. Malan, K. Suluksna, and E. Juntasaro. "Calibrating the gamma-Re,theta Transition Model for Commercial CFD". In: *47th AIAA Aerospace Sceinces Meeting* 1142 (2009).

[11] K.W. Mcalister, L.W. Carr, and W.J. Mccroskey. *Dynamic stall experiments on the NACA 0012 airfoil*. Tech. rep. 1100. NASA, 1978.

[12] J. Roskam. *Airplane Flight Dynamics and Automatic Flight Controls*. Ed. by Darcorporation. 1995.

[13] T. Theodorsen. "General Theory of Aerodynamic Instability and the Mechanism of Flutter". In: *National Advisory Committee for Aeronautics* (1935).

[14] M. Tobak. *On the Use of the Indicial Function Concept in the Analysis of Unsteady Motions of Wings and Wing-tail Combinations*. U.S. National Advisory Committee for Aeronautics, 1954.

[15] H. Wagner. "über die Entstehung des dynamischen Auftriebes von Tragflügeln". In: *ZAMM - Journal of Applied Mathematics and Mechanics* 5 (1925), pp. 7–35.